Available online at www.sciencedirect.com
ScienceDirect
Journal of Photochemistry and Photobiology A: Chemistry 189 (2007) 211–217
Journal of Photochemistry and Photobiology A:Chemistry
www.elsevier.com/locate/jphotochem

Dependence of photoionization quantum yield of indole and tryptophan in water on excitation wavelength

Ryuzi Katoh *

National Institute of Advanced Industrial Science and Technology (AIST), Tsukuba Central 5, 1-1-1 Higashi, Tsukuba, Ibaraki 305-8565, Japan

Received 5 December 2006; received in revised form 19 January 2007; accepted 31 January 2007
Available online 3 February 2007

Abstract

Excitation wavelength dependence (λ_{ex} = 220–290 nm) of photoionization quantum yields (Φ_{ion}) of indole and tryptophan in water were directly obtained through nanosecond time-resolved transient absorption measurements. Monophotonic photoionization occurred efficiently in this wavelength range. We conclude that photoionization proceeds through electron transfer from the neutral excited state to water by comparing the Φ_{ion} versus λ_{ex} dependences with the ground-state spectra. Mechanism of the electron transfer process is discussed.

Keywords: Photoionization; Transient absorption; Indole; Tryptophan

1. Introduction

Photoionization of molecules is an important photochemical reaction. When an isolated molecule in a vacuum absorbs a photon having sufficient energy for ionization, an energetic electron is emitted from the molecule into the vacuum with a high quantum yield [1]. In contrast, photoionization of a molecule in the condensed phase is significantly different from that in the gas phase because of interactions between charged species and surrounding molecules [2].

Because the various experimental techniques for studying photoionization (photoconductivity, transient absorption spectroscopy, and electron paramagnetic resonance spectroscopy) are typically performed with nonpolar solvents, the photoionization process of a molecule in the condensed phase has been studied in detail in nonpolar solvents such as liquid alkanes [2–8] and rare-gas liquids [9]. Upon photoexcitation of a molecule in a nonpolar solvent, an energetic electron is emitted from a parent molecule to the conduction band of the solvent. Subsequently, the emitted electron and surrounding molecules collide efficiently, and ultimately the electron is thermalized in the Coulomb field induced by the parent cation. Then the electron and the parent cation geminately recombine very efficiently. Although primary quantum yield is expected to be high, the quantum yield of photoionization in nonpolar solvents evaluated through steady-state photoconductivity measurements [3] was found to be small ($<10^{-1}$). The geminate recombination model was confirmed by the dependence of the electric field on photoconduction [3,4] and by using ultrafast transient absorption spectroscopy [5]. The threshold energy has been determined through photoconductivity measurements [6]. Threshold energies in the condensed phase are much lower than those in the gas phase and this difference can be explained as the stabilization due to polarization of solvent molecules and the energy position of the conduction band of the solvent. The threshold energy has been carefully compared with the theoretical model [7]. Additionally, the pressure effect has also been examined [8]. From these observations, the photoionization process of a molecule in a nonpolar solvent can be regarded as a direct ionization (DI) process, namely, generation of energetic electrons.

For polar solvents, such as alcohol and water, the photoionization process is significantly affected by orientation polarization. The stabilization energy for generated charged species induced by orientation polarization is much larger than that for electronic polarization. Also, many trap sites in the solvent conduction band are formed by density fluctuation of the solvent. The photoionization process of molecules has also been studied for organic polar solvents such as ethers [10], alcohols [11], and nitriles [12–14]. In such solvents, photoionization occurs with longer wavelength light irradiation [10]. Formation of a

* Tel.: +81 29 861 4840; fax: +81 29 861 5301.
E-mail address: r-katoh@aist.go.jp.

1010-6030/$ – see front matter © 2007 Elsevier B.V. All rights reserved.
doi:10.1016/j.jphotochem.2007.01.034

long-lived ion pair has been observed [11] instead of fast geminate recombination, suggesting that the initial recombination process is different from that in nonpolar solvents.

To understand the effect of orientation polarization on the photoionization process, one must take into account the time-dependent response of the orientation polarization. Photoionization of a molecule is a very fast process, and therefore molecular orientation cannot entirely follow the event, suggesting that the threshold energy in polar solvents is similar to that in nonpolar solvents. However, photoionization with low-energy photon irradiation has been observed with high quantum yield for a polar solvent system. This finding was explained on the basis of the concept of pre-existing trap sites for electrons formed by density fluctuation of the solvent [15]. In this model, solvated electrons are generated by electron transfer to the trap sites from the excited state (ET process). Accordingly, the threshold energy for the production of a solvated electron in a polar solvent is expected to be lower than that for the production of energetic electrons (DI process).

The characteristic feature of photoionization in polar solvents should be clearly observed in water because water has an extremely large static dielectric constant ($\varepsilon_{static} = 80$), with only a small contribution of electronic polarization (about 2% of ε_{static}). Although the photoionization process in water is not fully understood, molecules in water are photoionized with a high quantum yield and with low photon energies [16–18]. For example, aniline in water is photoionized with a quantum yield of 0.18 with 266-nm photon irradiation [16]. These observations suggest that photoionization of molecules in water proceeds not only by the DI process but also by the ET process.

The photoionization of biological molecules in water is an important primary process for photodamage of molecules in biological systems. Thus, the photoionization and photophysical processes of indole [17–19] and tryptophan [20–23] in water have been studied extensively as prototypes, but mechanistic details remain unresolved. In nanosecond time-resolved transient absorption measurements, a high quantum yield (0.27 at 266 nm) of photoionization of indole in water was observed [17], whereas a low quantum yield was observed with tryptophan (0.05 at 266 nm), which has a similar molecular structure [22]. These observations imply that the ET process is included in the photoionization process.

To study the ET process, the photoionization action spectrum should be compared with the ground-state absorption spectrum. However, the action spectrum is difficult to obtain experimentally. For a nonpolar solvent system, photoconductivity measurements using a ultra violet (UV) lamp and a synchrotron radiation (SR) light source can be applied for this purpose [2–4], but for a polar solvent system, high dark current disturbs the measurements. Use of an indirect alternative technique such as product analysis after photoirradiation has been examined, but quantitative discussion is difficult.

For indole and tryptophan, excitation wavelength dependence of the production yield of solvated electrons has been studied through the analysis of chemical products generated by capturing solvated electrons [19–21]. Bernas et al. estimated the threshold energy of solvated electron production to be 4.35 eV (285 nm) and the quantum yield to be 0.045 at 250 nm (4.95 eV) for indole [19]. They found that the quantum yield monotonously increased with increasing photon energy. The quantum yield of photoionization is much lower than that estimated through transient absorption spectroscopy (0.27 at 266 nm [17]). For tryptophan, reported spectra [20,21] are different among researchers. Although the reason for this discrepancy is unclear, direct evaluation through transient absorption spectroscopy would be preferable because artifacts due to side reactions can be eliminated.

Here we use nanosecond time-resolved transient absorption spectroscopy to evaluate the photoionization quantum yields of indole and tryptophan in water as a function of excitation wavelength from 220 to 290 nm. In the present measurements, the quantum yield of photoionization after the fast geminate recombination can be evaluated. By comparing these dependences with the ground-state absorption spectra of the molecules, we discuss photoionization via the ET process.

2. Experimental

Indole (Aldrich) and tryptophan (D-tryptophan, Nakarai) were used as received. Water (Nakarai, HPLC grade) was used as solvent without further purification. The concentration of the sample solutions was typically 5 mM. At this concentration, the exciting light pulse (<290 nm) was perfectly absorbed in a cell having a 1-cm path length. Steady-state absorption was measured for diluted solutions with an absorption spectrophotometer (Shimadzu, UV–VIS 2200).

For the transient absorption measurements, variable excitation light pulses (220–290 nm) were generated by the second harmonic of an optical parametric oscillator (Spectra Physics, MOPO-SL) excited by a Nd^{3+}:YAG laser (Spectra Physics, Pro-230-10). The pulse duration of the laser was about 8 ns. A semiconductor laser (Neo-Arc, 5 mW, 670 nm) was used as the probe light source. The sample was excited through a pin-hole (3 mm in diameter) placed in front of the cell. The probe light was collinear with the excitation pulse and transferred through the pin-hole. The transmitted probe light was detected with a photodiode (Hamamatsu, S1722). The signal from the detector was amplified with an amplifier (NF Electronic Instruments, BX-31A) and processed with a digital oscilloscope (Tektronix, TDS680C). The intensity of the laser pulse was measured with a pyroelectric energy meter (Ophir, PE25). All measurements were carried out at 295 K.

3. Results

Fig. 1 shows the transient absorption signals of indole and tryptophan in water under 290-nm excitation ($\lambda_{obs} = 670$ nm). According to previous transient absorption measurements for indole [17] and tryptophan [22], absorptions due to excited triplet states and cations are negligibly small at 670 nm. Thus, the long-lived species in Fig. 1 can be assigned to solvated electrons in water, which have a peak at 720 nm.

The decay rate increases with increasing exciting light intensity, indicating that the decay of the transient absorption is

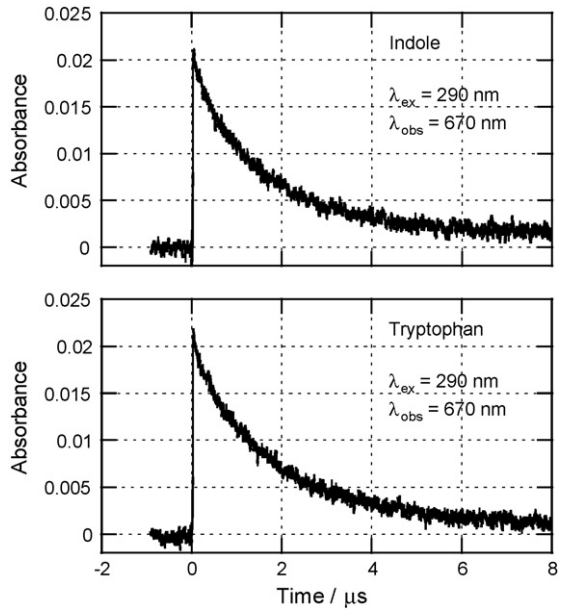

Fig. 1. Transient absorption signals of indole and tryptophan in water under 290-nm excitation observed at 670 nm.

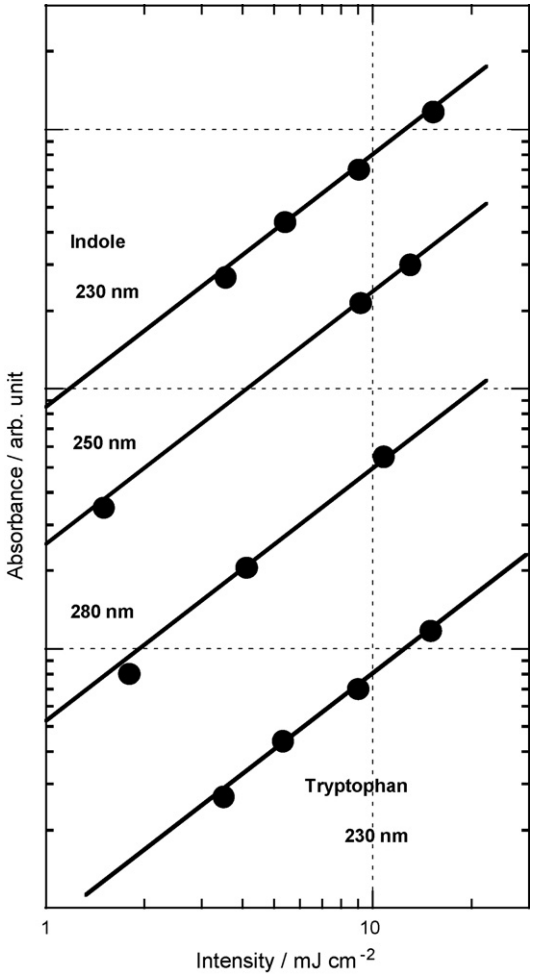

Fig. 2. Absorbance of indole and tryptophan due to solvated electrons as a function of exciting light intensity.

governed by bimolecular recombination between cations and solvated electrons. Because the concentrations of the solutions in Fig. 1 were adjusted to give the same absorbance at 290 nm, identical absorbance changes just after excitation clearly indicate that the same concentration of electrons was produced in each solution. Under this condition, the decay profiles for the solutions are the same, indicating identical bimolecular recombination rate constants. The rate of bimolecular recombination of tryptophan in water proceeds at the diffusion limit [22]. Thus the bimolecular recombination rate constant of the indole solution also proceeds at the diffusion limit. Although the absolute values of the rate constants can be evaluated from the observed decay profiles in principle, they are difficult to obtain under the present experimental conditions. The probe light was collinear with the excitation pulse which is absorbed completely in the sample solution in the cell, namely the density of generated species is not homogeneous along the depth of the cell. Thus, the decay profile deviates from the second order kinetics.

For indole in water, Kohler and co-workers studied the primary process for photoionization directly by using femtosecond time-resolved measurements [18]. They observed no geminate recombination up to 100 ps. This finding implies that recombination between an electron and a cation is not diffusion limited, suggesting the existence of a barrier for the recombination reaction. However, as discussed above, the secondary (bulk) recombination between indole cations and solvated electrons is diffusion limited, which suggests that a barrier exists only during the early time stage. Probably, the barrier arises by reorientation of surrounding water molecules coupling with excited indole molecules.

Fig. 2 plots absorbance just after excitation as a function of exciting light intensity. Transient absorption signals were observed at 230, 250, and 280 nm for the indole solution and at 230 nm for the tryptophan solution. The transient absorption signals due to the production of solvated electrons are proportional to the exciting light intensity. This result clearly indicates that photoionization occurs through a monophotonic process, which is consistent with previous studies for indole [17,18] and tryptophan [22,23].

Figs. 3 and 4 show the quantum yield of photoionization as a function of excitation wavelength together with the ground-state absorption spectrum for indole and tryptophan, respectively. The quantum yield was determined directly from the absorbance just after excitation and the exciting light intensity using the value of the absorption coefficient ($\varepsilon = 17{,}500\ M^{-1}\ cm^{-1}$) of solvated electron at 670 nm [24].

Although there are no reports for the wavelength dependence of the quantum yield of photoionization of indole and tryptophan in water through transient absorption spectroscopy, absolute values of the quantum yield have been evaluated at particular excitation wavelength. For indole, Saito et al. estimated the quantum yield to be 0.27 at 266 nm (4.66 eV) [17]. For tryptophan, Stevenson et al. estimated the photoionization quantum yield to be 0.05 at room temperature under 266-nm (4.66 eV) excitation [22]. These values are similar to our results, suggesting that transient absorption spectroscopy is reliable technique

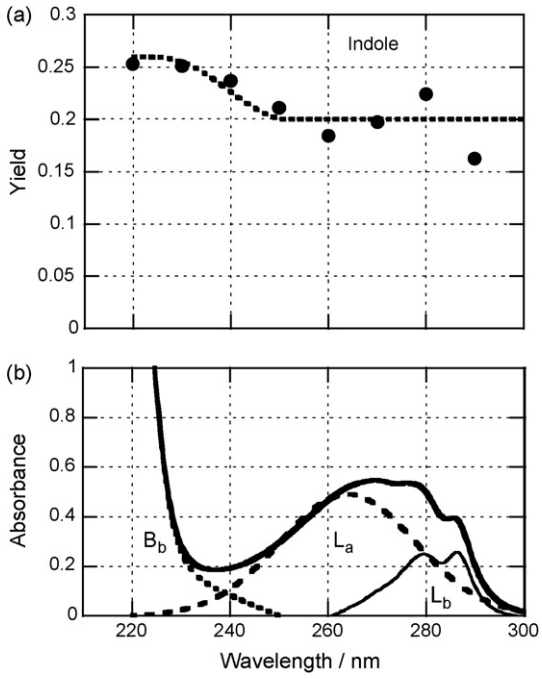

Fig. 3. Quantum yield of photoionization of indole in water (a) and ground-state absorption spectrum (b). The dotted line in (a) represents the model based on the ET process via the excited state. The thin solid line, dashed line, and dotted line in (b) represent the contributions of the L_b, L_a, and B_b states to the absorption spectrum (thick solid line).

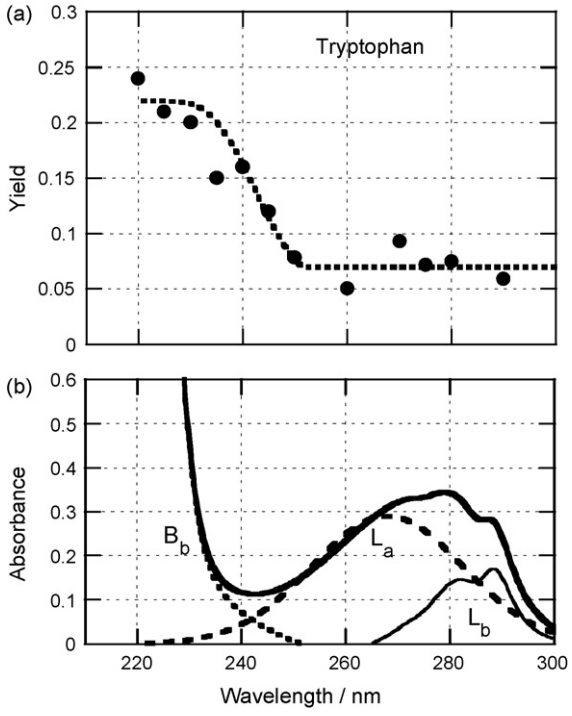

Fig. 4. Quantum yield of photoionization of tryptophan in water (a) and ground-state absorption spectrum (b). The dotted line in (a) represents the model based on the ET process via the excited state. The thin solid line, dashed line, and dotted line in (b) represent the contributions of the L_b, L_a, and B_b states to the absorption spectrum (thick solid line).

for the quantitative evaluation of the quantum yield of photoionization.

Excitation wavelength dependence of the quantum yield of the photoionization of these molecules in water has been studied through product analysis. For indole, Bernas et al. found that the quantum yield monotonously increased with increasing photon energy and estimated the threshold energy to be 4.35 eV (285 nm) through product analysis [19]. They also estimated the quantum yield to be 0.045 at 250 nm (4.95 eV). For tryptophan, the shape of the spectrum is different among researchers [20,21]. The absolute values of the efficiency are also reported, for example to be 0.012 at 270 nm (4.59 eV) [20]. These results are significantly different from our results. Although the reason for this discrepancy is unclear, direct evaluation by transient absorption spectroscopy is essential for quantitative discussion. This is because artifacts due to side reactions can be eliminated.

4. Discussion

4.1. Threshold energy for the production of the energetic electron (DI process)

To discuss the contribution of the direct ionization (DI) process in the action spectra for the photoionization shown in Fig. 3, we estimate the threshold energy for the production of the energetic electron from the molecule to the liquid based on the theoretical model, which is fulfilled for nonpolar solutions [2,7]. The threshold energy can be expressed as [2,7]

$$I_P^L = I_P^G + P_+ + V_0 \quad (1)$$

where I_P^G is the ionization potential of a molecule in the gas phase, P_+ the polarization energy induced by a cation, and V_0 is the conduction band energy of the liquid. According to the Born model, the polarization energy P_+ can be written as

$$P_+ = -\frac{e^2}{8\pi\varepsilon_0 R}\left[1 - \left(\frac{1}{\varepsilon}\right)\right] \quad (2)$$

where R is the effective radius of the ion, e the elementary charge, ε the dielectric constant of the medium, and ε_0 is the permittivity of the vacuum. Eqs. (1) and (2) give reasonable values for the threshold energy of photoionization of molecules in liquid alkanes when the van der Waals radius [25] R_{vdW} is used as the effective radius R of the ion [7].

To estimate the threshold energy of the DI process in water, one must carefully evaluate the dielectric constant of water because it strongly depends on the frequency of the motion of the charge. If a generated charge moves slowly, the rotational motion of water molecules in a medium follows the motion of the charge completely. Thus, the static dielectric constant of water ($\varepsilon_{static} = 80$), which is mainly due to orientation polarization, can be used for the evaluation. In contrast, for a rapidly moving charged species, such as an energetic electron, molecular motion is effectively frozen, and therefore only electronic polarization can contribute to stabilization. Under this condition, the optical dielectric constant (ε_{opt}) should be used; ε_{opt} is

related to the square of the refractive index n^2 because electronic polarization is dominant. For liquid water, $\varepsilon_{opt} = n^2 = 1.8$.

Photoelectron emission from the surface of liquid water is useful for evaluating the value of the effective dielectric constant for the DI process. During photoelectron emission, energetic electrons are emitted from the surface to vacuum. The threshold energy I_{PE}^{L} can be obtained by changing the wavelength of the excitation light or the analysis of the kinetic energy of emitted electrons. The difference $I_{PE}^{L} - I_{P}^{G}$ gives the polarization energy for the event:

$$P_+ = I_{PE}^{L} - I_{P}^{G} \quad (3)$$

The polarization energy obtained in Eq. (3) can be used in Eq. (2) to estimate the effective dielectric constant for the generation of an energetic electron.

Ogawa et al. evaluated the polarization energy through photoelectron emission from the molecules on the water surface. They estimated the value of P_+ to be −0.95 eV for perylene on water [26]. From this energy, an effective dielectric constant $\varepsilon = 2.2$ can be obtained. Recently, Winter et al. studied the photoemission spectrum of liquid water [27]. They pointed out that the effective dielectric constant is similar to the optical dielectric constant ($\varepsilon = 1.8$) estimated from the stabilization energy. This finding clearly shows that the dielectric constant during the DI process can be considered to be that at high frequency; that is, the square of the refractive index n^2 can be used to estimate the polarization energy.

For indole in water, the threshold energy of photoionization can be evaluated by the above-mentioned procedure. The polarization energy can be estimated to be $P_+ = -1.1$ eV using the square of the refractive index ($n^2 = 1.8$) and an estimated van der Waals radius of $R_{vdW} = 3.0$ nm. The conduction band energy has been reported to be $V_0 = -1.2$ eV [24], and the ionization potential of indole in the gas phase is $I_{P}^{G} = 7.76$ eV [17]. Therefore the threshold energy of the DI process for indole in water can be estimated to be I_{P}^{L} (Ind) = 5.5 eV (225 nm) by using Eq. (2). For tryptophan, the threshold energy should be similar to that for indole because the π-conjugated part, that is, the indole unit, determines the ionization potential.

On the basis of the foregoing considerations, for indole and tryptophan in water, generation of solvated electrons from energetic electrons (DI process) is not expected for excitation wavelengths longer than 225 nm (5.5 eV); however, one-photon generation of solvated electrons is observed at wavelengths longer than 225 nm (Figs. 3a and 4a). This finding suggests that solvated electrons are produced by electron transfer (ET process) from the excited-state molecule to the acceptor site of the solvent at excitation wavelengths longer than 225 nm.

4.2. Mechanism of photoionization via the excited state (ET process)

To discuss photoionization via the excited state (ET process), the photoionization action spectrum should be compared with the ground-state absorption spectrum. The ground-state absorption spectra of indole and tryptophan in the wavelength range 220–290 nm consist of contributions from three states, namely, the L_a, L_b, and B_b states. Recently, Jalviste and Ohta reported electric field modulated absorption spectra of indole in poly(methyl methacrylate) (PMMA) films [28]. They analyzed the spectra in the wavelength range between 230 and 310 nm in terms of three bands. The lowest absorption band corresponds to the L_b state and has vibrational structure. The second band corresponds to the L_a state, and its broadened spectrum can be fitted by Gaussian functions. The third highest state is observed below 250 nm and is assigned to the B_b state, which increases monotonously with wavelength. The spectrum of indole in water (Fig. 3b) is similar to that in PMMA except for broadening of vibrational structure at the longer wavelength side.

On the basis of the analysis of the ground-state absorption spectrum reported by Jalviste and Ohta [28], we analyzed our spectrum for indole in water in terms of three states. First, we assumed that the absorption band corresponding to the L_a state of indole could be represented by a single Gaussian function (dashed line in Fig. 3b). Subtracting this component from the complete absorption spectrum yielded the contribution of the L_b and B_b states, which are shown as a thin solid line and a dotted line in Fig. 3b, respectively. At longer wavelengths (>250 nm), both the L_a and L_b states contribute to the absorption spectrum, and around 260 nm, the contribution of the L_a state is dominant. At wavelengths shorter than 250 nm, the contribution of the B_b state becomes pronounced. We analyzed the absorption spectrum for tryptophan in water by the same procedure (Fig. 4b).

The photoionization quantum yield seems constant for both indole (Fig. 3a) and tryptophan (Fig. 4a) solutions at wavelengths longer than 250 nm. In contrast, at wavelengths shorter than 250 nm, the quantum yield increases with decreasing wavelength for both solutions. The onset wavelengths correspond to the onset of absorption due to the B_b state in each solution. The constant quantum yield at longer wavelengths (>250 nm) suggests the same quantum yield of electron-transfer reaction upon excitation of the L_a and L_b states, and the steep increase at shorter wavelengths (<250 nm) suggests an increase in the relative contribution of the B_b state, which is an efficient channel for electron transfer. On the basis of these considerations, the dependence of the photoionization quantum yield on the excitation wavelength can be reproduced as the dotted lines in Figs. 3a and 4a. For these calculations, we assumed the following quantum yields of photoionization (Φ_{ion}) via L_a, L_b, and B_b: for indole, L_a, 0.2; L_b, 0.2; B_b, 0.26; for tryptophan, L_a, 0.07; L_b, 0.07; B_b, 0.22. There are three characteristic features of the wavelength dependence: (1) the quantum yields via the L_a and L_b states of indole ($\Phi_{ion} = 0.2$) are much larger than those of tryptophan ($\Phi_{ion} = 0.07$); (2) the quantum yield via the L_a state is the same as that via the L_b state; and (3) the quantum yield via the B_b state is larger than that via the L_a and L_b states.

From the foregoing, it is apparent that photoionization occurs by the ET process when the neutral excited state is populated. We shall now discuss about the fact that quantum yields via L_a and L_b for indole were much larger than those for tryptophan. For the ET process, electrons are transferred from the excited molecule to the solvent, probably to the pre-existing trap sites formed by the

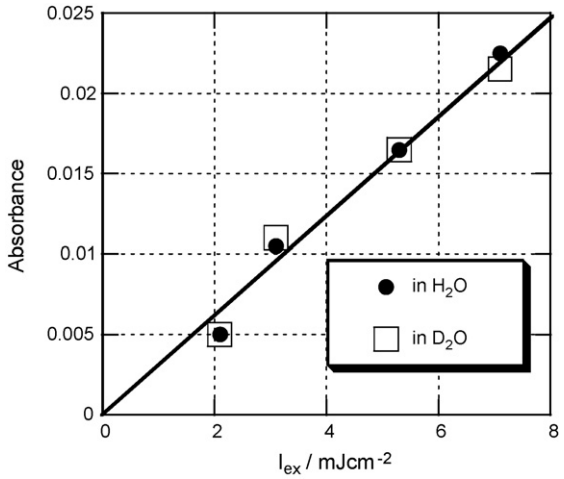

Fig. 5. Effect of deuteration on the photoionization quantum yield: initial absorbance change due to solvated electron production as a function of excitation intensity.

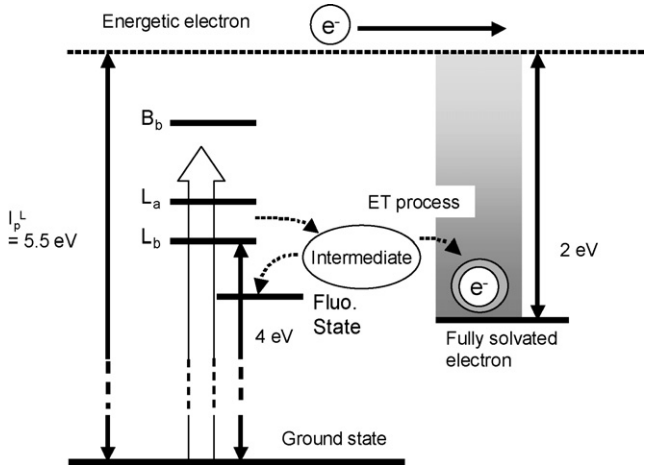

Fig. 6. Schematic diagram of the photoionization process.

density fluctuation of the surrounding molecules. Accordingly, two factors should be considered in a detailed discussion of the ET mechanism: the structure of surrounding water molecules organized by the specific intermolecular interaction between a solute molecule and surrounding molecule, and the electronic structure of the excited molecule itself. Highly quantum yield is achieved if the solvent structure is favorably organized by the intermolecular interaction for the electron transfer. Hydrogen bond is likely for the formation of the favorable solvent structure. Recently, Yago et al. reported that the reorganization energies for photo-induced electron transfer reactions were affected by hydrogen bonding [29]. This suggests that the favorable solvent structure would be formed by hydrogen bond. Highly quantum yield is also achieved if the electronic coupling between an excited solute molecule and the pre-existing trap site is strong enough. Rydberg-like structure is likely for the strong electronic coupling.

To investigate the structure of surrounding water molecules organized by hydrogen bond, we compared the transient absorption of indole in D_2O with that of indole in H_2O (Fig. 5). No difference was observed, suggesting that there is no favorable structure organized by hydrogen bond. Thus, we consider that the electronic structure of the excited molecule itself is the key to determine the quantum yield via the ET process.

Saito et al. have studied the photoionization process of aniline derivatives including indole in water excited by 308- and 266-nm light [17]. The quantum yields in Saito's study were different for various solute molecules. This finding is similar to the trend of the present results; namely, the quantum yields via L_a and L_b for indole were much larger than those for tryptophan. According to Saito et al., the quantum yields are not correlated with the ionization potentials I_P^G of the solute molecules in the gas phase but are well correlated with the formal charge on the N atom in the cation state. This result implies that Φ_{ion} is sensitive to the electronic structure of the molecules itself.

On the basis of the foregoing considerations, we schematically present the ET process in Fig. 6. As discussed above, the energy required for the production of an energetic electron can be estimated to be 5.5 eV. The neutral excited states – L_a, L_b, and B_b – are located below the free-electron state. The energy level of a fully solvated electron is located about 2 eV below the free-electron state estimated from the transition energy of a fully solvated electron to the free-electron state [30]. This fact clearly means that electron transfer from the lowest excited state of indole to the solvent is energetically possible. Although photoionization of indole in water occurs with excitation in the lowest excited state with a 4.1-ns lifetime, generation of solvated electrons in water occurs in the femtosecond time range [18]. This fact clearly indicates that the ET process does not occur from the fluorescent state. Specifically, production of solvated electrons occurs through a short-lived intermediate state located near the lowest excited state populated by an internal conversion process from Franck-Condon state. The short-lived intermediate state can also relax to the stable fluorescent state.

We now discuss the origin of the intermediate state. Recently, Sobolewski et al. pointed out the importance of the $^1\pi\sigma^*$ state of indole for understanding the nonradiative decay process [31]. The $^1\pi\sigma^*$ state is located slightly above the lowest excited state and has a Rydberg-like character localized on the N atom, which would have relatively strong electronic coupling with the pre-existing trap sites formed by the density fluctuation of the surrounding water molecules. Thus, the $^1\pi\sigma^*$ state can be considered to be a candidate for the intermediate state for the ET process. Because the optical transition from the ground state to the $^1\pi\sigma^*$ state has a small oscillator strength [31], the $^1\pi\sigma^*$ state is probably populated through optically allowed excited states, namely, the L_a, L_b, and B_b states, by an internal conversion process. The L_a, L_b, and B_b states as well as the $^1\pi\sigma^*$ state relax to the fluorescent state. In Fig. 6, these relaxation channels are depicted by the arrows (dotted line). The photoionization quantum yield is determined by the branching ratio between these channels. Thus, the larger photoionization quantum yields of indole by comparing with that of tryptophan under the L_a- and L_b-state excitation condition is due to the efficient internal conversion to the $^1\pi\sigma^*$ state, which is sensitive to the energy

positions of the L_a and L_b states or efficient photoionization reaction of the $^1\pi\sigma^*$ state.

As already pointed out, the quantum yield via the L_a state is the same as that via the L_b state in both solutions. This fact implies that the internal conversion efficiency from the L_a state to the $^1\pi\sigma^*$ state is the same as that from the L_b state. The reason for this similar quantum yield is not clear at present. One possibility is that internal conversion to the $^1\pi\sigma^*$ state occurs after state mixing of the L_a and L_b states, which has been suggested through ultrafast fluorescence spectroscopy [32]. When the B_b state is populated, the photoionization quantum yield increases. There are two possibilities for the higher quantum yield. One is due to large branching ratio relaxing to the same intermediate state ($^1\pi\sigma^*$ state) as for the L_a and L_b states and the other is due to coupling of the B_b state with higher lying intermediate state having Rydberg-like structure. An increase in the quantum yield at higher photon energy irradiation was observed for photoionization of aniline derivatives [17] and for the photodetachment of halide anion by charge-transfer to solvent (CTTS) band excitation [33,34].

Recently, photoionization of DNA bases in water has been studied. Although the photoionization quantum yield is not high, photoionization occurs under UV (220–300 nm) excitation [35,36]. The base molecules of DNA have an ionization potential in the gas phase similar to that of indole (7.76 eV) [37]. Thus, photoionization through the DI process is not expected. Accordingly, the excited-state properties of the intermediate state play an important role in photochemical reactions in biological systems.

5. Conclusion

Photoionization quantum yields of indole and tryptophan in water were evaluated as a function of excitation wavelength from 220 to 290 nm through nanosecond time-resolved transient absorption measurements. For the entire wavelength range studied, solvated electrons were produced through a monophotonic process. We have discussed the energy required for the generation of energetic electrons based on the polarization model and concluded that energetic electrons are not ejected from molecules in the wavelength range studied. Thus, we considered that electron transfer from the excited state (ET process) is the dominant process. The dependence of the quantum efficiency on the excitation wavelength was reproduced by using a simple model; namely, different excited states have different quantum yields. In comparing our results with previous reports, we consider that the electronic structure of the excited molecule itself is the key to determine the quantum yield via the ET process.

Acknowledgement

This work was partly supported by a Grant-in-Aid for Scientific Research (Project 18045033, Priority Area 452) from the Ministry of Education, Culture, Sports, Science and Technology (MEXT) of Japan.

References

[1] A. Mozumder, Y. Hatano, Charged Particle and Photon Interactions with Matter, Marcel Dekker, New York, 2004, p. 105.
[2] W.F. Schmidt, Liquid State Electronics of Insulating Liquids, CRC Press, Boca Raton, FL, 1997.
[3] H.T. Choi, D.S. Sethi, C.L. Braun, J. Chem. Phys. 77 (1982) 6027–6039.
[4] D.W. Tweeten, S. Lipsky, J. Phys. Chem. 93 (1989) 2683–2688.
[5] Y. Hirata, N. Mataga, J. Phys. Chem. 95 (1991) 1640–1644.
[6] R.A. Holroyd, J.M. Preses, E.H. Böttcher, W.F. Schmidt, J. Phys. Chem. 88 (1984) 744–749.
[7] R. Katoh, K. Lacmann, W.F. Schmidt, Z. Phys. Chem. 190 (1995) 193–201.
[8] R. Katoh, K. Lacmann, W.F. Schmidt, Chem. Phys. 195 (1995) 457–463.
[9] K. Nakagawa, Radiat. Phys. Chem. 37 (1991) 643–651.
[10] Y. Nakato, M. Ozaki, H. Tsubomura, J. Phys. Chem. 76 (1972) 2105–2112.
[11] Y. Hirata, N. Mataga, J. Phys. Chem. 87 (1983) 3190–3192.
[12] Y. Hirata, N. Mataga, J. Phys. Chem. 87 (1983) 1680–1682.
[13] C. Xia, J. Peon, B. Kohler, J. Chem. Phys. 117 (2002) 8855–8866.
[14] P. Jacques, X. Allonas, A. Sarbach, E. Haselbach, E. Vauthey, Chem. Phys. Lett. 378 (2003) 185–191.
[15] M. Hilczer, M. Tachiya, J. Chem. Phys. 100 (1996) 7691–7697.
[16] F. Saito, S. Tobita, H. Shizuka, J. Chem. Soc., Faraday Trans. I 92 (1996) 4177–4185.
[17] F. Saito, S. Tobita, H. Shizuka, J. Photochem. Photobiol. A 106 (1997) 119–126.
[18] J. Peon, G.C. Hess, J.-M.L. Pecourt, T. Yuzawa, B. Kohler, J. Phys. Chem. A 103 (1999) 2460–2466.
[19] A. Bernas, D. Grand, E. Amouyal, J. Phys. Chem. 84 (1980) 1259–1262.
[20] H.B. Steen, J. Chem. Phys. 61 (1974) 3997–4002.
[21] E. Amouyal, A. Bernas, D. Grand, Photochem. Photobiol. 29 (1979) 1071–1077.
[22] K.L. Stevenson, G.A. Papadantonakis, P.R. LeBreton, J. Photochem. Photobiol. A 133 (2000) 159–167.
[23] P.S. Sherin, O.A. Snytnikova, Y.P. Tsentalovich, Chem. Phys. Lett. 391 (2004) 44–49.
[24] CRC Handbook of Radiation Chemistry, CRC Press, Boca Raton, FL, 1991.
[25] J.T. Edward, J. Chem. Educ. 47 (1970) 261–270.
[26] T. Ogawa, H. Chen, T. Inoue, K. Nakashima, Chem. Phys. Lett. 229 (1994) 328–332.
[27] B. Winter, R. Weber, W. Widdra, M. Dittmar, M. Faubel, I.V. Hertel, J. Phys. Chem. A 108 (2004) 2625–2632.
[28] E. Jalviste, N. Ohta, J. Chem. Phys. 121 (2004) 4730–4739.
[29] T. Yago, Y. Kobori, K. Akiyama, S. Tero-Kubota, Chem. Phys. Lett. 369 (2003) 49–54.
[30] F.-Y. Jou, G.R. Freeman, Can. J. Chem. 57 (1979) 591–597.
[31] A.L. Sobolewski, W. Domcke, C. Dedonder-Lardeux, C. Jouvet, Phys. Chem. Chem. Phys. 4 (2002) 1093–1100.
[32] X. Shen, J.R. Kuntson, J. Phys. Chem. B 105 (2001) 6260–6265.
[33] A. Iwata, N. Nakashima, M. Kusaba, Y. Izawa, C. Yamanaka, Chem. Phys. Lett. 207 (1993) 137–142.
[34] M.C. Sauer Jr., R.A. Crowell, I.A. Shkrob, J. Phys. Chem. A 108 (2004) 5490–5502.
[35] C.E. Crespo-Hernández, R. Arce, J. Phys. Chem. B 107 (2003) 1062–1070.
[36] S. Marguet, D. Markovitsi, F. Talbot, J. Phys. Chem. B 110 (2006) 11037–11039.
[37] H. Sugiyama, I. Saito, J. Am. Chem. Soc. 118 (1996) 7063–7068.